

Performance Analysis of Novel Multi-band Photonic-integrated WSS Operated on 400ZR

Original

Performance Analysis of Novel Multi-band Photonic-integrated WSS Operated on 400ZR / Khan, Ihtesham; Tunesi, Lorenzo; Masood, Muhammad Umar; Ghillino, Enrico; Carena, Andrea; Bardella, Paolo; Curri, Vittorio. - ELETTRONICO. - (2022), pp. 1-2. (Intervento presentato al convegno IEEE Summer Topicals Meeting Series (SUM) tenutosi a Cabo San Lucas, Mexico nel 11-13 July 2022) [10.1109/SUM53465.2022.9858263].

Availability:

This version is available at: 11583/2970750 since: 2022-08-24T21:06:03Z

Publisher:

IEEE

Published

DOI:10.1109/SUM53465.2022.9858263

Terms of use:

This article is made available under terms and conditions as specified in the corresponding bibliographic description in the repository

Publisher copyright

IEEE postprint/Author's Accepted Manuscript

©2022 IEEE. Personal use of this material is permitted. Permission from IEEE must be obtained for all other uses, in any current or future media, including reprinting/republishing this material for advertising or promotional purposes, creating new collecting works, for resale or lists, or reuse of any copyrighted component of this work in other works.

(Article begins on next page)

Performance Analysis of Novel Multi-band Photonic-integrated WSS Operated on 400ZR

Ihtesham Khan
Politecnico di Torino, IT
ihtesham.khan@polito.it

Lorenzo Tunesi
Politecnico di Torino, IT
lorenzo.tunesi@polito.it

Muhammad Umar Masood
Politecnico di Torino, IT
muhammad.masood@polito.it

Enrico Ghillino
Synopsys, Inc., USA
enrico.ghillino@synopsys.com

Andrea Carena
Politecnico di Torino, IT
andrea.carena@polito.it

Paolo Bardella
Politecnico di Torino, IT
paolo.bardella@polito.it

Vittorio Curri
Politecnico di Torino, IT
curri@polito.it

Abstract—We present a detailed performance analysis of a novel photonic integrated wide-band wavelength selective switch operating in S+C+L bands. The results demonstrate that the proposed device offers low loss and frequency flat behavior for the considered band in a single or cascade implementation.

Index Terms—Ultra-wideband, Photonic Integrated Circuits, Wavelength-selective Switch

I. INTRODUCTION

The introduction of 5G technology and the Internet of Things (IoT) concept revolutionaries the network speed and connectivity but creates new challenges in terms of bandwidth requirements. The present optical transport exploits dual-polarization coherent transmission technologies and Wavelength-Division Multiplexing (WDM) in the C-band. The primary aim of the network operator is to exploit the residual capacity of the already deployed infrastructure and provide bandwidth resources to accommodate the requirements of these new technologies. In this context, Multi-Band Transmission (MBT) is a cost-effective solution to deliver additional optical spectrum by utilizing the existing infrastructure. The fundamental block for implementing the MBT system requires scalable switching solutions to carry out Ultra-Wideband (UWB) operations. To this end, Photonic Integrated Circuits (PICs) provide a cost-effective solution with a small footprint and broad range of bandwidth capabilities. This work analyzes the performance of the novel, modular and scalable UWB Wavelength-Selective Switch (WSS) compatible with the silicon photonic platform covering the S+C+L bands. The performance analysis is demonstrated on the transmission and network level for a single or cascade implementation.

II. WAVELENGTH SELECTIVE SWITCH

The proposed WSS has the capabilities of routing independently M channels to one of the target N output ports while avoiding any internal routing conflict. The overall design is based on a multi-stage structure that separates the filtering and switching operation, reducing the circuit complexity. The schematic can be seen in **Fig. 1a**, together with the highlight of the two main sections of the architecture. The channel filtering is achieved through a cascade of filters tasked with separating

the operating bands and mitigating the inter-channel cross-talk and aliasing. The switching operation is then carried out by M parallel $1 \times N$ switching networks, which route the signal to the target output port. The proposed architecture Quality-of-Transmission (QoT) has been investigated for $M = 30$ channels, considering $N = 3$ possible output ports. From the device standpoint, the bands' separation filters have been implemented as contra-propagating couplers [1], allowing a large flat bandwidth of operation. In contrast, the channel filters in the second cascade have been implemented as two-stage ladder Micro-Ring Resonators (MRR) [2]. The switching operation is achieved through thermally controlled Mach-Zehnder Interferometers (MZI) designed for the three main operation windows.

III. PERFORMANCE ANALYSIS OF WSS

The transmission performance of the proposed UWB WSS has been characterized by considering the coherent transmission setup in the OptSim[®]. The transmission parameters related to 400ZR standard [3] has been considered (dual-polarization 16QAM modulation and a symbol rate $R_S=60$ GBaud), with a channel spacing of FSR=100 GHz. The Optical Signal-to-Noise Ratio penalty (Δ OSNR) has been considered as the evaluating parameter for transmission impairments. This metric has been obtained by simulating the Bit-Error Rate (BER) for all the possible configurations of the device, using a reference BER threshold $BER_{th} = 10^{-3}$ [4]. The proposed WSS has a relatively flat response, and the path-dependent penalty is mainly associated with the encountered waveguide crossings. The distribution of crossing encounters depends both on the channel under consideration as well as the target output fiber required, as shown in **Fig. 1b**. As depicted in the figure, the interconnect are combined into five main groups, allowing a reduction of the number of encountered crossings with respect to un-grouped topologies, which represents the critical element affecting the scalability of this architecture. The crossing distribution also exhibits symmetry with respect to the first and last target output fibers: this is due to the symmetric nature of the device grouping and the equal number of channels per operation band. The obtained OSNR penalties

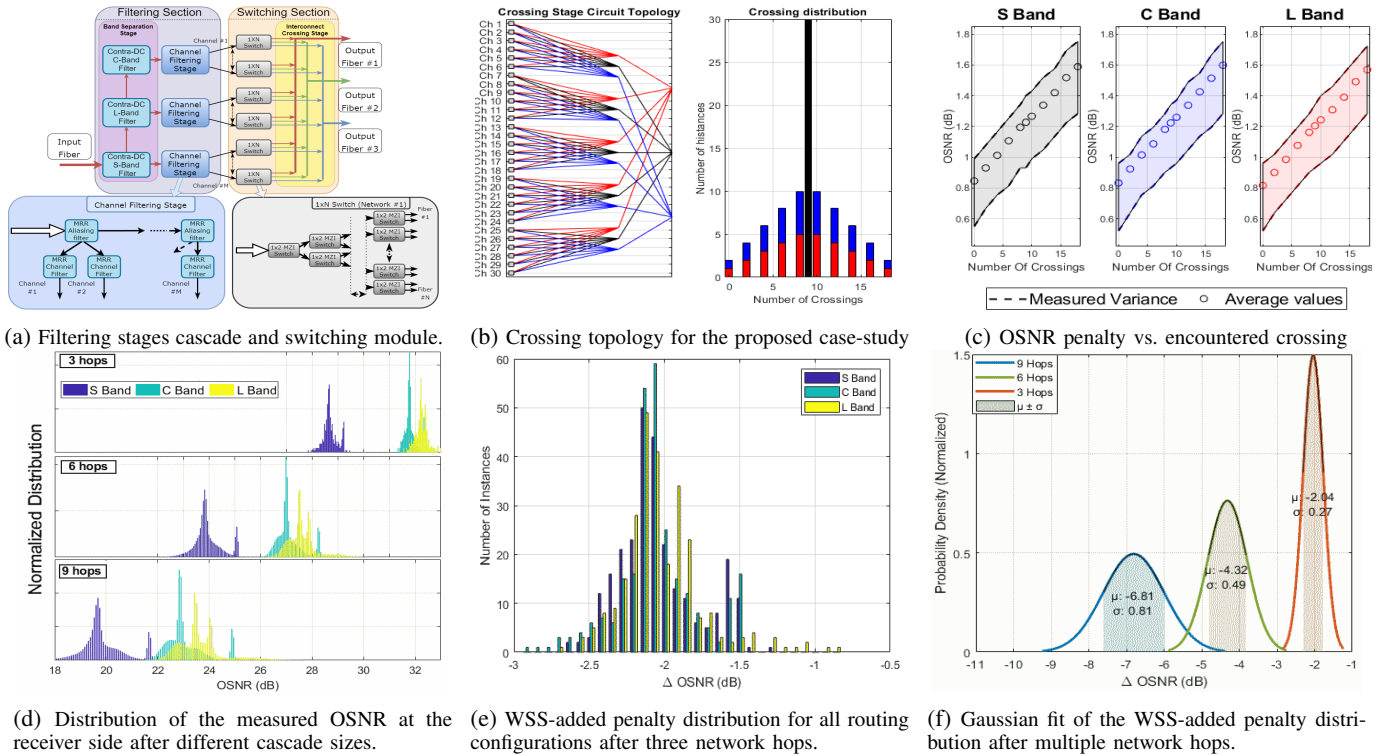


Fig. 1: Wavelength selective switch schematic and detailed performance analysis

are presented as a function of crossings in **Fig. 1c** where the average value among all channels is highlighted together with the measured minimum and maximum values. This linear dependence in **Fig. 1c** confirms the leading role of the waveguide interconnects in determining the configuration penalty with respect to the flat degradation of filtering and switching elements.

To further analyze the performance of the proposed WSS, a point-to-point system with an arbitrary number of WSS stages N_{stages} is simulated. The system receiver end collects the data from all the possible paths that each channel can traverse at each stage. Any given channel can be routed to three different target WSS devices of the following stage, allowing a total number of $N_{\text{config}} = 3^{N_{\text{stages}}}$ configurations for each individual channel. Each stage of the proposed framework is connected by Optical Lines Systems (OLSs) with the same fiber type and proper amplifier type based upon the band of operation. The parameters for the OLSs reported in [5] for each operating band are considered in this analysis. The proposed simulation scenario only considers the standard fiber losses and linear part of the impairments, i.e., the amplified spontaneous emission (ASE) noise. The cumulative Light-Path (LP) OSNR at each given stage can be evaluated as $\text{OSNR}^{-1} = \sum_{i=1}^{N_{\text{stages}}} \frac{1}{\text{OSNR}_i}$.

The proposed framework has been simulated in transparency; the power loss by the fiber are fully compensated by the amplifier ($P_{\text{in}} = P_o = 0$ dBm). The penalty introduced by the WSS elements has been considered from transmission-level simulation, which enables a more precise evaluation without approximating the switching penalty to a single average value. The distribution of OSNR in the three operating

bands measured at the receiver is shown in **Fig. 1d** for three different network scenarios, corresponding to a 3, 6, and 9 stages WSS cascade, respectively. The general QoT in **Fig. 1d** is frequency-dependent, but this is primarily due to the different OLS parameters applied in the S, C and L bands. The penalty introduced by the WSS is relatively independent of the frequency bands (see **Fig. 1e**) due to the tailored design of the physical elements. Furthermore, in **Fig. 1f** the ΔOSNR distribution is shown for each considered case, with a highlight on the standard deviation $\sigma_{\Delta\text{OSNR}}$ boundaries: for the 3-hops structure we obtain $\mu_{\Delta\text{OSNR}} = -6.81$ dB and $\sigma_{\Delta\text{OSNR}} = 0.81$ dB, for the 6-hops structure we obtain $\mu_{\Delta\text{OSNR}} = -4.32$ dB and $\sigma_{\Delta\text{OSNR}} = 0.49$ dB, while for the 9-hops circuit $\mu_{\Delta\text{OSNR}} = -2.04$ dB and $\sigma_{\Delta\text{OSNR}} = 0.27$ dB.

This work reveals the performance analysis of a modular photonic integrated UWB WSS that supports a wide scale of the optical spectrum, including the S+C+L bands. The results demonstrate that the proposed device offers low loss and frequency flat behavior for the considered bands in a single or cascade operation.

REFERENCES

- [1] M. Hammood *et al.*, "Broadband, silicon photonic, optical add-drop filters with 3 dB bandwidths up to 11 THz," *Opt. Lett.* **46**, 2738–2741 (2021).
- [2] A. P. Masilamani *et al.*, "Design and realization of a two-stage microring ladder filter in silicon-on-insulator," *Opt. Lett.* **20**, 24708–24713 (2012).
- [3] <https://www.oiforum.com/technical-work/hot-topics/400zr-2/>.
- [4] I. Khan *et al.*, "Performance evaluation of data-driven techniques for software and agnostic management of N×N photonic switch," *Opt. Continuum* **1** (2022).
- [5] B. Correia *et al.*, "Power control strategies and network performance assessment for C+L+S multiband optical transport," *JOCN* **13**, 147–157 (2021).